SUPREX (Stability of Unpurified Proteins from Rates of H/D Exchange) Analysis of the Thermodynamics of Synergistic Anion Binding by Ferric-Binding Protein (FbpA), a Bacterial Transferrin†

Petra L. Roulhac,‡,§ Kendall D. Powell,‡,§,|| Suraj Dhungana,‡,⊥ Katherine D. Weaver,‡ Timothy A. Mietzner,# Alvin L. Crumbliss,‡ and Michael C. Fitzgerald*,‡

Department of Chemistry, Duke University, Durham, North Carolina 27708, and Department of Molecular Genetics and Biochemistry, University of Pittsburgh, Pittsburgh, Pennsylvania 15261

Received August 22, 2004; Revised Manuscript Received September 28, 2004

ABSTRACT: SUPREX (stability of unpurified proteins from rates of H/D exchange) is a H/D exchange- and matrix-assisted laser desorption/ionization (MALDI)-based technique for characterizing the equilibrium unfolding/refolding properties of proteins and protein−ligand complexes. Here, we describe the application of SUPREX to the thermodynamic analysis of synergistic anion binding to iron-loaded ferric-binding protein (Fe^{3+}FbpA−X, X = synergistic anion). The *in vivo* function of FbpA is to transport unchelated Fe^{3+} across the periplasmic space of certain Gram-negative bacteria, a process that requires simultaneous binding of a synergistic anion. Our results indicate that Fe^{3+}FbpA−X is not a so-called "ideal" protein system for SUPREX analyses because it does not exhibit two-state folding properties and it does not exhibit EX2 H/D exchange behavior. However, despite these nonideal properties of the Fe^{3+}FbpA−X protein-folding/unfolding reaction, we demonstrate that the SUPREX technique is still amenable to the quantitative thermodynamic analysis of synergistic anion binding to Fe^{3+}FbpA. As part of this work, the SUPREX technique was used to evaluate the $\Delta\Delta G_f$ values of four synergistic anion-containing complexes of Fe^{3+}FbpA (i.e., Fe^{3+}FbpA−PO_4, Fe^{3+}FbpA−citrate, Fe^{3+}FbpA−AsO_4, and Fe^{3+}FbpA−SO_4). The $\Delta\Delta G_f$ value obtained for Fe^{3+}FbpA−citrate relative to Fe^{3+}FbpA−PO_4 (1.45 ± 0.44 kcal/mol), is in good agreement with that reported previously (1.98 kcal/mol). The value obtained for Fe^{3+}FbpA−AsO_4 (0.58 ± 0.45 kcal/mol) was also consistent with that reported previously (0.68 kcal/mol), but the measurement error is very close to the magnitude of the value. This work (i) demonstrates the utility of the SUPREX method for studying anion binding by FbpA, (ii) provides the first evaluation of a $\Delta\Delta G_f$ value for Fe^{3+}-FbpA−SO_4, −1.43 ± 0.17 kcal/mol, and (iii) helps substantiate our hypothesis that the synergistic anion plays a role in controlling the lability of iron bound to FbpA in the transport process.

SUPREX (stability of unpurified proteins from rates of H/D exchange)[1] is a new mass spectrometry-based technique for making thermodynamic measurements of protein stability. We and others have previously demonstrated the utility of the SUPREX technique for evaluating protein-folding free energies (ΔG_f values), protein-folding *m* values, and the binding affinities of protein−ligand complexes (*1*−*8*). The technique affords several unique experimental advantages over conventional methods for making such thermodynamic measurements on proteins and protein−ligand complexes. These advantages include speed, sensitivity, and the ability to analyze both highly purified protein samples as well as protein samples in complex biological mixtures such as those found *in vivo*.

To date, all of the proteins and protein−ligand complexes that have been subject to quantitative thermodynamic analyses by SUPREX have been so-called "ideal" protein systems. Ideal protein systems for SUPREX analyses include those systems in which the protein-folding reaction is well-modeled by a two-state (folded and unfolded) process and in which the protein is under EX2 exchange conditions (i.e., the folding rate of the protein is much faster than the intrinsic exchange rate of an unprotected amide proton). For many proteins, it is possible to create EX2 exchange conditions with the right choice of buffer pH, because protein-folding rates are often insensitive to modest pH changes, whereas intrinsic exchange rates of unprotected amide protons are very sensitive to pH (*9*). However, the two-state folding requirement of SUPREX has largely limited the applicability

† This work was supported by a National Science Foundation PECASE Award to M.C.F. (CHE-00−94224) and a National Science Foundation grant to A.L.C. (CHE-00-79066).

* To whom correspondence should be addressed: Department of Chemistry, Box 90346, Duke University, Durham, NC 27708-0346. Telephone: 919-660-1547. Fax: 919-660-1605. E-mail: michael.c.fitzgerald@duke.edu.

‡ Duke University.

§ These authors made equal contributions to this work.

|| Present Address: Icoria, Inc., Durham, North Carolina 27709.

⊥ Present Address: Los Alamos National Laboratory, Los Alamos, New Mexico 87545.

University of Pittsburgh.

[1] Abbreviations: SUPREX, stability of unpurified proteins from rates of H/D exchange; MALDI, matrix-assisted laser desorption/ionization; TFA, trifluoroacetic acid; CD, circular dichroism; FbpA, ferric-binding protein; Fe^{3+}FbpA, iron-loaded ferric-binding protein; PO_4, phosphate anion; Cit, citrate anion; AsO_4, arsenate anion, SO_4, sulfate anion; MES, 4-morpholineethanesulfonic acid; GdmCl, guanidinium chloride.

10.1021/bi0481848 CCC: $27.50
Published on Web 11/23/2004

of the technique to the analysis of relatively small (<20 kDa) proteins. While it is clear that such two-state folding behavior is required for the accurate determination of ΔG_f and *m* values by SUPREX, it is less clear what effect nontwo-state folding behavior will have on the determination of $\Delta\Delta G_f$ values in SUPREX experiments on a given protein system. Here, we investigate the SUPREX behavior of a model nonideal protein system, the ferric-binding protein (FbpA).

FbpA is a 34-kDa protein responsible for the transport of unchelated iron across the periplasmic space of certain Gram-negative bacteria (*10*). To achieve the tight Fe^{3+} sequestration necessary to accomplish this task, FbpA requires simultaneous binding of a synergistic anion. Consequently, FbpA is classified as a bacterial transferrin because of both the nature of its iron-binding properties and its overall function. In contrast to mammalian transferrin, FbpA is a single lobe protein with an Fe^{3+}-binding site defined by His-9, Glu-57, Tyr-195, and Tyr-196 (*11*). In recombinant *Haemophilus influenzae* and *Neisseria gonorrhoreae* FbpA isolated from *Escherichia coli*, the fifth and sixth Fe^{3+} coordination sites are occupied by a synergistic PO_4 anion and H_2O (*11*, *12*). Although this observation suggests that PO_4 is the preferred synergistic anion *in vivo*, it has been observed that several anions can satisfy the synergistic anion requirement for tight Fe^{3+} binding (*13*−*16*). Synergistic anion exchange is relatively facile and is found to modulate protein affinity for Fe^{3+} binding as well as the protein-bound Fe^{3+}/Fe^{2+} redox potential (*14*). Furthermore, in addition to the thermodynamic and structural roles of the synergistic anion, we find that it plays a kinetic role in the *in vitro* Fe^{3+} loading and unloading processes (*17*, *18*). Recently, we have also hypothesized that FbpA may play an *in vivo* role in addition to periplasmic iron transport, that of polyphosphate hydrolysis (*16*). Anions clearly play a crucial role in iron loading and unloading by FbpA.

Periplasmic iron transport is important in bacterial life cycles because iron is an essential nutrient and iron acquisition is critical to the survival of bacteria. Because the periplasm is rich in anion diversity (*19*) and because a possible role of FbpA involvement in polyphosphate anion hydrolysis is emerging (*16*), we are developing methods to explore the interactions of iron-loaded FbpA (Fe^{3+}FbpA) and synergistic anions that are applicable *in vitro* and *in vivo*. In this paper, we explore the application of the SUPREX technique to a thermodynamic characterization of anion binding to the Fe^{3+}FbpA complex. In addition to providing insight into an important biochemical process, the Fe^{3+}-FbpA−X system (X = synergistic anion) provides an important test of the applicability of the SUPREX technique to the quantitative analysis of protein−ligand-binding interactions involving "non-ideal" protein systems for SUPREX analyses (i.e., systems in which the protein-folding reaction is not two-state and the protein under study is not under EX2 exchange conditions).

MATERIALS AND METHODS

Instrumentation. Circular dichroism (CD) and fluorescence spectroscopy experiments were performed using a PiStar-180 CDF spectrometer from Applied Photophysics equipped with a temperature-controlled cell holder. This instrument was also equipped with an automatic titration system to facilitate data collection in the guanidine-induced denaturation/renaturation experiments described below. MALDI (matrix-assisted laser desorption/ionization) mass spectra were acquired on a Voyager DE Biospectrometry Workstation from Perseptive Biosystems. Positive ion mass spectra were collected in the linear mode using a nitrogen laser (337 nm, 3 Hz). Guanidinium chloride (GdmCl) concentrations were determined using a Bausch and Lomb refractometer (*20*). Measurements of pH were made with a Jenco 6072 pH meter equipped with a Futura calomel pH electrode from Beckman Instruments. To correct for isotope effects, the pH of each D_2O solution was converted to a pD by adding 0.4 to the measured pH value (*21*).

Isolation and Purification of FbpA. Purified apo-FbpA, cloned from *N. gonorrhoreae* and expressed in *E. coli*, was prepared as previously reported (*13*, *22*). Briefly, *E. coli* overexpressing FbpA was subjected to extraction by cetyltrimethyammonium bromide extraction in 0.1 M Tris base at pH 8.0, followed by binding to a carboxymethyl sepharose column. While bound to the column, iron-loaded FbpA was converted to apo-FbpA by the addition of 10 volumes of 0.1 M Tris base at pH 8.0 containing 1 mM citrate. Elution of apo-FbpA was accomplished using a NaCl gradient in buffers rendered iron free by exposure to Chelex 100 (BioRad) prior to their addition to the column. Fractions were collected in acid-washed glassware and extensively dialyzed against Chelex 100-treated 0.05 M 4-morpholineethanesulfonic acid (MES) (Sigma−Aldrich) buffer containing 0.2 M KCl and concentrated using an Amicon filtration unit.

Preparation of Fe^{3+}FbpA Complexes. Fe^{3+}FbpA−AsO_4 was prepared as previously described (*14*). For Fe^{3+}FbpA−Cit and Fe^{3+}FbpA−PO_4, 1.2 equiv of citrate or 10 equiv of phosphate at pH 6.5 was added to 1 equiv of apo-FbpA. After gentle mixing for 30 min, 1.2 equiv of $FeCl_2$ was added and mixing was continued for an additional 30 min. For Fe^{3+}-FbpA−SO_4, 1.5 equiv of $FeSO_4$ was added to a 1 molar equiv of apo-FbpA, followed by gentle mixing for 30 min. All four Fe^{3+}FbpA complexes were stored overnight in solution at 4 °C, and excess iron in the form of insoluble $Fe(OH)_3$ was removed using a syringe driven 0.8 mM filter unit (Millex, Millpore). The filtrate was then dialyzed 3 times at 4 °C against 0.05 M MES/0.2 M KCl for 2 h each starting at pH 6.5 and ending at pH 6.5 or 4.5, depending on the experiment.

The final concentration of iron-loaded protein stock solution was determined using the absorbance value at 474 nm (ϵ = 1770 M^{-1} cm^{-1}) for Fe^{3+}FbpA−Cit, at 481 nm (ϵ = 2430 M^{-1} cm^{-1}) for Fe^{3+}FbpA−PO_4, at 476 nm (ϵ = 2280 M^{-1} cm^{-1}) for Fe^{3+}FbpA−AsO_4, and at 495 nm (ϵ = 2460 M^{-1} cm^{-1}) for Fe^{3+}FbpA−SO_4 (*13*, *14*, *16*). All spectra were obtained using a Cary 100 Bio UV−visible spectrophotometer (Varian) at 25.0 ± 0.1 °C. The final concentration of iron-loaded protein in the above stock solutions was typically 150−450 μM. The above iron-loaded protein stock solutions were diluted to 100−150 μM before use in CD and SUPREX experiments.

Conventional Equilibrium Unfolding Studies. Guanidine-induced equilibrium unfolding and refolding data for Fe^{3+}-FbpA−PO_4 were collected using both fluorescence and far-UV-CD as structural probes for the unfolding/refolding reaction. These experiments involved the preparation of stock solutions of folded and unfolded Fe^{3+}FbpA−PO_4. The folded

stock solution contained Fe^{3+}FbpA−PO_4 at a concentration of 6 μM in a buffer solution containing 10 mM MES and 40 mM KCl at pH 6.5. The unfolded stock solution was comprised of Fe^{3+}FbpA−PO_4 (6 μM), guanidine (5.8 M), and a buffer containing 10 mM MES and 40 mM KCl at pH 6.5. Note that the protein concentrations and buffer compositions of the stock solutions containing folded and unfolded protein were identical with the exception that the unfolded stock solution contained 5.8 M guanidine. Denaturation curves were obtained by titration of the folded protein stock solution with the unfolded protein stock solution. Renaturation curves were recorded by titration of the unfolded protein stock solution with the folded protein stock solution.

The far-UV-CD denaturation/renaturation curves were collected by recording the CD signal (i.e., the ellipticity in millidegrees) of the protein at 222 nm as a function of the denaturant concentration. The fluorescence denaturation/renaturation curves were collected by recording the total fluorescence signal obtained using an excitation wavelength of 280 nm and an emission filter with an optical cutoff of 305 nm. Both fluorescence and CD signal measurements were made at denaturant concentrations ranging from 0 to 5.8 M guanidine at 0.1 M increments. The data points in each denaturation/renaturation curve represent the signal obtained after the protein was equilibrated at each denaturant concentration for 10 min. In separate experiments, it was determined that this 10-min equilibration time was sufficient for the Fe^{3+}FbpA−PO_4 system to reach equilibrium in the denaturant-containing buffer system employed in this work.

SUPREX Analyses. The SUPREX data in this work were collected and analyzed according to previously established protocols (*3*, *6*, *7*). Briefly, SUPREX analyses were initiated by the 10-fold dilution of 1-μL aliquots of the appropriate Fe^{3+}FbpA−X stock solution into a series of H/D exchange buffers. Two sets of H/D exchange buffers were used in this work. One set contained 50 mM MES, 200 mM KCl, and increasing concentrations of GdmCl at pD 6.5, and a second set contained 50 mM MES, 200 mM KCl, and increasing concentrations of GdmCl at pD 4.5.

After dilution of the Fe^{3+}FbpA−X complex into each series of exchange buffers, the resulting solutions were incubated at room temperature (293 K) and allowed to exchange for a specified amount of time. This amount of time was the same for each point in a given SUPREX curve (see below). After the specified time, the H/D exchange reactions were quenched and the deuterium content of the protein in each buffer was determined by MALDI mass spectrometry. In some cases, the H/D exchange reactions were quenched by direct dilution (5−10-fold) into the MALDI matrix solution and then subjected to a MALDI mass spectral analysis. In other cases, the H/D exchange reactions were quenched with the addition of trifluoroacetic acid (TFA, final concentration 0.3% v/v), and the protein samples in each H/D exchange reaction were submitted to a concentration and desalting step using C4 ZipTips (Millipore, Inc.) prior to MALDI mass spectral analysis. The concentration and desalting step was performed as previously described (*7*).

A single MALDI sample of the protein in each H/D exchange buffer was prepared, and 5−10 replicate MALDI mass spectra were acquired for each MALDI sample. The protein molecular weight determinations from these 5−10 replicate MALDI mass spectra were then used to determine the number of deuterons that had exchanged into the protein (i.e., a Δmass value). ΔMass values were determined by subtracting the molecular weight of the fully protonated FbpA protein (i.e., 33 597.9 Da) from the molecular weight of the protein ascertained in each MALDI analysis. Ultimately, an average Δmass value of the protein was determined for the protein in each GdmCl-containing H/D exchange buffer, and this value was used to generate SUPREX curves (i.e., plots of Δmass versus [GdmCl]) at specific exchange times.

Multiple SUPREX curves for the Fe^{3+}FbpA−X samples in this study were generated using H/D exchange times that varied between 1 and 52 h. The data points in each SUPREX curve were used to extract a $C_{SUPREX}^{1/2}$ value (i.e., the denaturant concentration at the transition midpoint). The $C_{SUPREX}^{1/2}$ values extracted from each SUPREX curve were plotted as a function of the H/D exchange time according to eq 1 as described by Powell and Fitzgerald (*6*). In eq 1, R is

$$RT \ln(\langle k_{int} \rangle t/0.693 - 1) = - mC_{SUPREX}^{1/2} - \Delta G \quad (1)$$

the gas constant, T is the temperature in Kelvin, $\langle k_{int} \rangle$ is the estimated average intrinsic exchange rate of an unprotected amide proton, t is the H/D exchange time used in SUPREX, m is defined as $\delta\Delta G/\delta$[denaturant], and ΔG is the folding free energy of the protein in the absence of denaturant. A linear least-squares analysis of the data was used to evaluate the slope and y intercept that correspond to the protein-folding m and ΔG values, respectively. The $\langle k_{int} \rangle$ values used in our calculations at pD 4.5 and 6.5 (29.4 and 2318.4 hr^{-1}, respectively) were determined using the SPHERE program (*9*, *23*) and the entire primary amino acid sequence of FbpA (*12*).

RESULTS AND DISCUSSION

Denaturant-Induced Equilibrium Unfolding Properties of Fe^{3+}FbpA−PO_4. The GdmCl-induced equilibrium unfolding and refolding curves for Fe^{3+}FbpA−PO_4 generated by fluorescence and CD are shown in Figure 1. The near coincidence of the unfolding and refolding curves shown in Figure 1 indicates that the GdmCl-induced unfolding reaction of Fe^{3+}FbpA−PO_4 is reversible under these experimental conditions (i.e., in a buffer containing 10 mM MES and 40 mM KCl at pH 6.5).

Generally, the coincidence of folding/unfolding transitions monitored by multiple structural probes can be used to support a two-state folding/unfolding model, and the noncoincidence of such transitions can be used to support a nontwo-state model of folding/unfolding. If the fluorescence and CD denaturation curves shown in parts A and B of Figure 1 are normalized to an apparent fraction of unfolded protein (i.e., F_{app}), the general shape and position of the two denaturation curves can be directly compared (see Figure 1C). Such a comparison reveals that the two curves are not coincident. This result suggests that the GdmCl-induced equilibrium unfolding reaction of Fe^{3+}FbpA−PO_4 is not well-modeled by a two-state process involving only folded and unfolded species. One or more partially folded intermediate states appear to be populated in the GdmCl-induced equilibrium unfolding reaction of Fe^{3+}FbpA−PO_4.

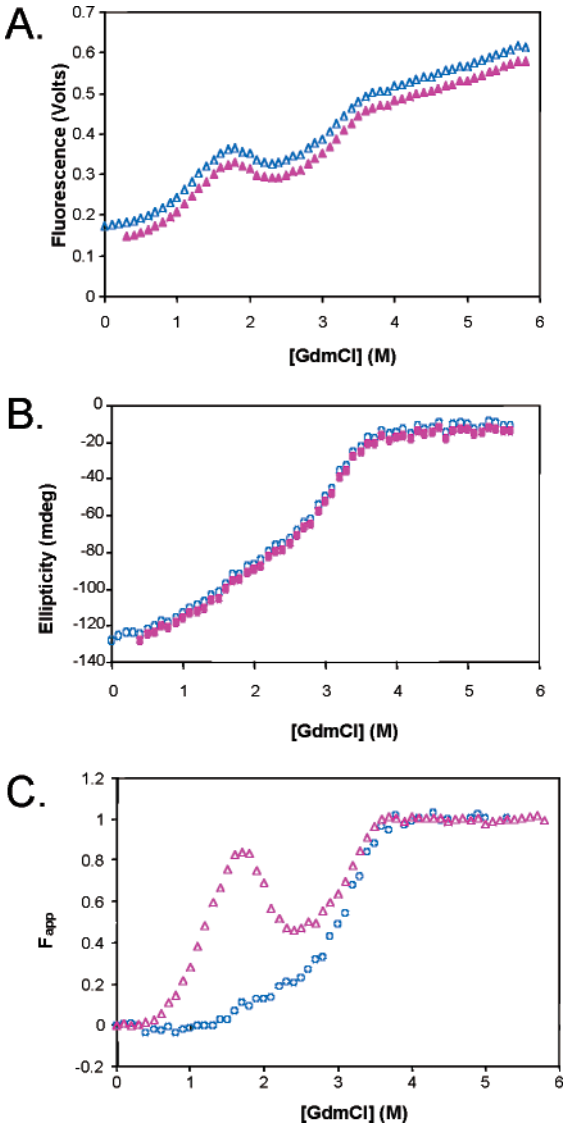

FIGURE 1: GdmCl-induced equilibrium unfolding of Fe^{3+}FbpA−PO_4 followed by both fluorescence and far-UV CD. (A) Raw fluorescence emission data was obtained with excitation at 280 nm and using an optical filter with a wavelength cutoff of 305 nm recorded at a protein concentration of 6 μM, forward (△) and reverse (▲). (B) Raw far-UV-CD signals that were recorded at a protein concentration of 6 μM, forward (○) and reverse (●). (C) Normalized fluorescence emission data (△) plotted on the same axis as the normalized far-UV-CD data (○).

SUPREX Analysis of Fe^{3+}FbpA−PO_4. The SUPREX behavior of Fe^{3+}FbpA−PO_4 was studied at pD 4.5 and 6.5. Shown in Figure 2A are the SUPREX data recorded for Fe^{3+}-FbpA−PO_4 at each pD using an H/D exchange time of 1 h. Four additional SUPREX curves were also recorded for the Fe^{3+}FbpA−PO_4 sample at each pH using a series of different H/D exchange times that ranged from 1 to 44 h (data not shown). A $C_{SUPREX}^{1/2}$ value (i.e., the concentration of denaturant at the transition midpoint) was extracted from each SUPREX curve generated (see Table 1). The $C_{SUPREX}^{1/2}$ values generated at each pD decreased when the H/D exchange time in the SUPREX experiment was increased.

We have previously shown that eq 1 can be used to describe the relationship between the $C_{SUPREX}^{1/2}$ value of a protein and the H/D exchange time used in a SUPREX experiment (*5*, *6*, *8*). In the case of "ideal" proteins for

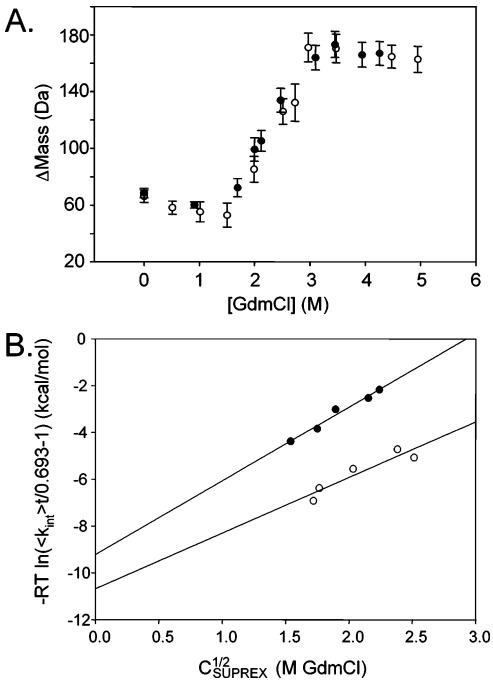

FIGURE 2: (A) SUPREX data obtained for Fe^{3+}FbpA−PO_4 at pD = 6.5 (○) and pD = 4.5 (●) using an H/D exchange time of 1 h. The error bars represent ±1 standard deviation. (B) $-RT\ \ln(\langle k_{int}\rangle t/0.693 - 1)$ versus $C_{SUPREX}^{1/2}$ plots obtained for Fe^{3+}FbpA−PO_4 at pD = 6.5 (○) and pD = 4.5 (●). H/D exchange times range from 1 to 44 h.

Table 1: Transition Midpoints (i.e., $C_{SUPREX}^{1/2}$ Values) Obtained for Fe^{3+}FbpA−PO_4 at pD 4.5 and 6.5

H/D exchange time (h)	$C_{SUPREX}^{1/2}$ at pD 4.5 [GdmCl] (M)[a]	$C_{SUPREX}^{1/2}$ at pD 6.5 [GdmCl] (M)[a]
1.00	2.24 ± 0.04	2.38 ± 0.09
1.83	2.15 ± 0.06	2.51 ± 0.07
4.18	1.90 ± 0.02	2.03 ± 0.07
17.27	1.75 ± 0.03	1.73 ± 0.03
43.80	1.54 ± 0.11	1.72 ± 0.20

[a] Errors are the standard error associated with fitting each SUPREX curve to a 4-parameter sigmoidal function in Sigma-Plot.

SUPREX analyses, eq 1 predicts that a plot of $RT\ \ln(\langle k_{int}\rangle t/0.693 - 1)$ versus $C_{SUPREX}^{1/2}$ will be linear and that the *y* intercept and slope of the resulting plot will correspond to the ΔG_f and *m* values, respectively, of the folding/unfolding reaction of the protein. "Ideal" protein systems in the SUPREX experiment are systems that exhibit reversible, two-state unfolding properties and that exhibit EX2 (and not EX1) exchange behavior.

EX1 exchange conditions exist when the folding rate of a protein is much slower than the intrinsic exchange rate of an unprotected amide proton (k_{int}), and two populations of H/D-exchanged molecules with two distinct masses are formed during the time course of the exchange reaction. One of these populations has a relatively low mass and includes H/D-exchanged molecules in which the unprotected amide protons of the protein have rapidly exchanged with solvent deuterons. The other population has a relatively high mass and includes H/D-exchanged molecules in which all of the amide protons of the protein have exchanged with solvent deuterons. This is in contrast to EX2 exchange behavior that occurs when the folding rate of the protein is much faster than the intrinsic exchange rate of an unprotected amide

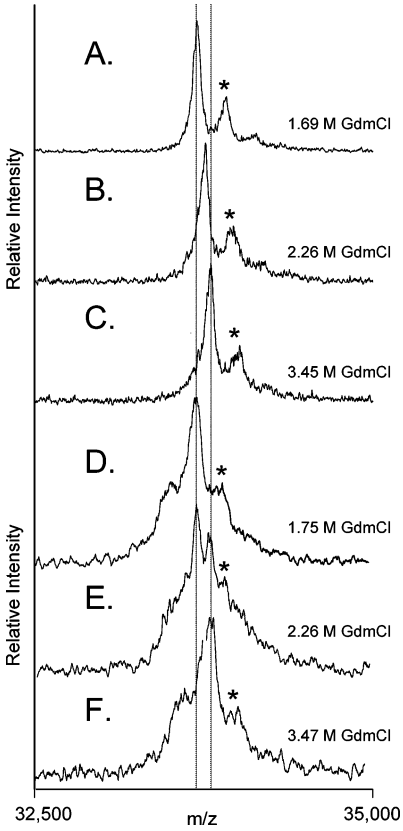

FIGURE 3: Representative MALDI−TOF mass spectra used to create the Fe^{3+}FbpA−PO_4 SUPREX curves shown in Figure 2. Typical mass spectra obtained to generate the Δmass values in the pretransition, transition, and post-transition regions of the pD 4.5 curve are shown in A, B, and C, respectively. Shown in D, E, and F are typical mass spectra obtained to generate the Δmass values in the pretransition, transition, and post-transition regions of the pD 6.5 curve. The dotted lines mark *m*/*z* values 33 671.3 and 33 772.1, which correspond to the average Δmass values of 72.4 and 173.2 Da, recorded in the pre- and post-transition baselines, respectively, of our SUPREX curves. Peaks marked with an asterisk correspond to matrix adducts.

proton (k_{int}). Under EX2 exchange conditions, the formation of only one population of H/D-exchanged protein molecules with one distinct mass is formed over the time course of the exchange reaction and the observed mass of this population increases with increasing exchange time. In many cases, the masses of the two populations of H/D molecules formed under EX1 exchange conditions can be resolved in the MALDI experiment. Therefore, the presence of two distinct protein ion signals in the mass spectral analysis of an H/D-exchanged protein is a hallmark of EX1 exchange behavior (*24*−*26*).

Shown in Figure 3 are representative MALDI mass spectra used to create the three major regions (i.e., the pretransition, transition, and post-transition regions) of the pD 4.5 and 6.5 SUPREX curves shown in Figure 2A. Note that a single population of H/D-exchanged protein molecules at *m*/*z* 33 717.6 is detected in the mass spectrum recorded in the transition region of the pD 4.5 SUPREX curve (i.e., the mass spectrum shown in Figure 3B); whereas, two distinct populations of H/D-exchanged protein molecules at *m*/*z* 33 670.9 and 33 770.9 are detected in the transition region of the pD 6.5 SUPREX curve (i.e., the mass spectrum shown in Figure 3E). The mass spectral results in Figure 3B are indicative of EX2 exchange behavior; and the mass spectral results in Figure 3E are indicative of EX1 exchange behavior. The reason for this difference in behavior with pD is that the H/D exchange rate of an unprotected amide proton, k_{int} in eq 1, is approximately 100-fold smaller at pD 4.5 than at 6.5. Because the protein folding and unfolding rates of FbpA are not expected to change significantly in going from pD 6.5 to 4.5 (see data in ref *17*), k_{int} becomes much smaller than the folding rate of the protein and therefore results in a change from EX1 to EX2 conditions.

In the case of EX2 exchange behavior, it is relatively straightforward to determine the requisite Δmass values for SUPREX analyses (i.e., there is only one protein ion signal to take into account). However, the determination of such Δmass values is complicated if the protein under study exhibits EX1 exchange behavior in the SUPREX experiment (i.e., there are two protein ion signals that must be taken into account). We note that the Δmass values used to construct the transition regions of the pD 6.5 SUPREX curves in this work were determined by making a center of mass calculation that included the protein ion signals from both populations of H/D-exchanged molecules.

It is interesting that only one population of H/D-exchanged molecules was observed in the mass spectra used to create the pre- and post-transition regions of both the pD 4.5 and 6.5 SUPREX curves. This is despite the apparent EX1 exchange behavior of the Fe^{3+}FbpA−PO_4 sample in the pD 6.5 buffer. In theory, the pre- and post-transition regions of the SUPREX curve of a protein should always be defined by a population of H/D-exchanged protein molecules with a single mass. In the pretransition region, this mass corresponds to the molecular weight of H/D-exchanged molecules in which the fast exchanging, unprotected amide protons of the protein have exchanged. This is because the H/D exchange reaction of the globally protected amide protons has not proceeded to any significant degree in the buffers used to generate the Δmass data in the pretransition baseline of a SUPREX curve. In the post-transition region of a SUPREX curve, all of the amide protons in the protein have been exchanged for solvent deuterons (the H/D exchange reaction is essentially over) and the observed mass of the H/D-exchanged molecules present corresponds to the molecular weight of protein molecules with essentially all of their amide protons exchanged for solvent deuterons. It is only in the transition region of a SUPREX curve that a meaningful measurement of the H/D exchange reaction of the globally protected amide protons of the protein is obtained. In the pretransition region, the reaction has not begun; in the post-transition region, the reaction is over; and at the $C_{SUPREX}^{1/2}$ value, the reaction is exactly half-over.

Interestingly, the $C_{SUPREX}^{1/2}$ values obtained in our SUPREX experiments on Fe^{3+}FbpA−PO_4 at pD 4.5 and 6.5 fit well to eq 1 (see Figure 2B). Correlation coefficients of 0.9875 and 0.9332 were obtained in our linear least-squares analysis of the data at pD 4.5 and 6.5, respectively. These relatively good correlations were observed despite the apparent nontwo-state folding/unfolding behavior and the apparent EX1 exchange behavior of this protein complex at pD 6.5 (see above). It is also noteworthy that the *y*-intercept and slope values obtained in our linear least-squares analysis of the pD 4.5 data in Figure 2B, -9.8 ± 0.9 kcal/mol and 2.3 ± 0.4 kcal/(mol M), respectively, were within experi-

mental error of the same values obtained in our linear least-squares analysis of the pD 6.5 data, -10.7 ± 1.1 kcal/mol and 2.4 ± 0.5 kcal/(mol M), respectively.

The *y*-intercept and slope values obtained in the above treatment of our SUPREX data cannot be an accurate reflection of the ΔG_f and *m* values of the folding reaction of Fe^{3+}FbpA$-PO_4$ at pD 4.5 and 6.5. Most importantly, these values were obtained assuming a two-state folding reaction, and the folding reaction of Fe^{3+}FbpA$-PO_4$ is clearly not two-state (see above). However, the above treatment of our SUPREX data does appear to provide a means by which to evaluate the *relative* folding properties of Fe^{3+}FbpA$-PO_4$ at the two pD values studied. In this respect, the similar *y*-intercept and slope values obtained in our SUPREX analysis of Fe^{3+}FbpA$-PO_4$ at pD 4.5 and 6.5 suggest that the overall folding behavior of Fe^{3+}FbpA$-PO_4$ is similar at the two pD values studied. This is consistent with the experimental data in ref *17* and with our experimental observation that the overall three-dimensional structure of Fe^{3+}FbpA$-PO_4$ is unchanged in going from pD 6.5 to 4.5 as judged by far-UV-CD spectroscopy (data not shown). Our results also suggest that the apparent EX1 exchange behavior of the Fe^{3+}FbpA$-PO_4$ complex at pD 6.5 did not preclude its SUPREX analysis at this pD. This is important because *in vivo* FbpA functions exclusively in the bacterial periplasmic space where the pH has been estimated to be slightly acidic (~6.5) (*19*).

SUPREX Analysis of Synergistic Anion Binding to Fe^{3+}FbpA. The above results indicate that it is possible to generate SUPREX curves for Fe^{3+}FbpA$-PO_4$, which can provide reasonably precise $C^{1/2}_{SUPREX}$ values, and most importantly that the H/D-exchange-time dependence of the $C^{1/2}_{SUPREX}$ values are well-described by eq 1. These findings prompted us to explore the utility of SUPREX for making quantitative thermodynamic measurements of synergistic anion binding to Fe^{3+}FbpA. We reasoned that the SUPREX-derived ΔG_f values of Fe^{3+}FbpA$-$X complexes containing different synergistic anions, X (e.g., Cit, AsO_4, PO_4, and SO_4), would be useful for quantifying the *relative* binding affinities of different synergistic anions to Fe^{3+}FbpA (i.e., for generating reasonably accurate and precise $\Delta\Delta G_f$ values). This is despite the inability of SUPREX to accurately define an absolute ΔG_f value for the Fe^{3+}FbpA$-$X folding/unfolding reaction. Our derivation of $\Delta\Delta G_f$ values in this manner assumes that the synergistic anions only interact with Fe^{3+}FbpA in its native, folded state.

A total of four Fe^{3+}FbpA$-$X complexes, differing only in the identity of the synergistic anion, were analyzed by SUPREX in this work. These complexes included the Fe^{3+}-FbpA$-PO_4$ complex described above and three additional Fe^{3+}FbpA$-$X complexes where the synergistic anion was AsO_4, Cit, or SO_4. SUPREX curves such as those shown in Figure 2 were obtained for each Fe^{3+}FbpA$-$X complex at pD 6.5 using a series of different H/D exchange times that ranged from 1 to 54 h. Ultimately, $C^{1/2}_{SUPREX}$ values were extracted from each curve and then plotted as a function of the H/D exchange time according to eq 1. The resulting $RT\ \ln(\langle k_{int}\rangle t/0.693 - 1)$ versus $C^{1/2}_{SUPREX}$ value plot for each complex is shown in Figure 4. The pD 6.5 data on the Fe^{3+}-FbpA$-PO_4$ complex in Figure 2B are replotted in Figure 4 for comparative purposes.

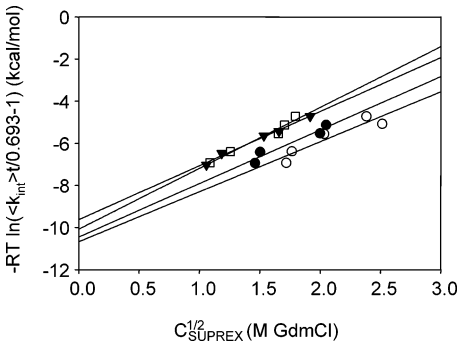

FIGURE 4: $-RT\ \ln(\langle k_{int}\rangle\ t/0.693 - 1)$ versus $C^{1/2}_{SUPREX}$ plots obtained for Fe^{3+}FbpA$-$X at pD = 6.5 where X = Cit (□), AsO_4 (●), PO_4 (○), or SO_4 (▼).

Equation 1 adequately describes the H/D-exchange-time dependence of the $C^{1/2}_{SUPREX}$ values that we obtained in our SUPREX experiments on all of the Fe^{3+}FbpA$-$X complexes that we studied (see Figure 4). Correlation coefficients for the four data sets plotted in Figure 4 ranged from 0.933 to 0.995. In each case, it was also possible to extract reasonably precise ΔG_f and *m* values from the data (see Table 2). In this analysis of the data, there did not appear to be a measurable difference between the SUPREX-derived ΔG_f and *m* values assigned to each complex.

The presence of different synergistic anions is not expected to impact the *m* value of Fe^{3+}FbpA$-$X protein-folding reactions as is observed in Table 2. The magnitude of the *m* value of a protein is largely defined by the number of species that are populated in the equilibrium unfolding/refolding reaction of a protein and by the difference in solvent-accessible surface area between the folded and unfolded state(s) (*27*). The binding of different synergistic anions is not expected to significantly change the species that are populated in the unfolding/refolding reaction of Fe^{3+}FbpA; and the binding interaction is not expected to bury a significant amount of hydrophobic surface area.

The presence of different synergistic anions is expected to change the thermodynamic stability of FbpA in the Fe^{3+}-FbpA$-$X complexes in our study. We have previously established the relative binding affinities of the synergistic anion in three of the four complexes studied here (*14*). Phosphate was determined to be the tightest binding synergistic anion, followed by arsenate and then citrate. Although there are only relatively small differences in the SUPREX-derived ΔG_f values in Table 2, it is interesting to note that the correct order of binding affinities (PO_4 > AsO_4 > Cit) can be assigned based on the magnitude of these values. What is also especially striking is the difference in the observed $C^{1/2}_{SUPREX}$ values obtained in our SUPREX experiments on Fe^{3+}FbpA$-PO_4$ and Fe^{3+}FbpA$-$Cit. This is highlighted in Figure 5, where the SUPREX curves obtained for the Fe^{3+}FbpA$-PO_4$ and Fe^{3+}FbpA$-$Cit complexes using an H/D exchange time of 1 h are plotted on the same graph. The SUPREX curves for these two complexes yielded $C^{1/2}_{SUPREX}$ values of 2.38 ± 0.09 and 1.79 ± 0.06, respectively (see Figure 5).

The difference in $C^{1/2}_{SUPREX}$ values between Fe^{3+}FbpA$-$ PO_4 and Fe^{3+}FbpA$-$Cit is clearly measurable in our SUPREX experiments on these two complexes. However, the ΔG_f values derived in Table 2 for these complexes are

Table 2: Summary of SUPREX-Derived Thermodynamic Parameters for the Fe^{3+}FbpA−Anion Complexes in This Study

anion in Fe^{3+}FbpA−X complex	ΔG_f[a] (kcal/mol)	m[a] (kcal/(mol M))	ΔG_{avg}[b] (kcal/mol)	SUPREX $\Delta\Delta G_{avg}$[c] (kcal/mol)	literature $\Delta\Delta G$[d] (kcal/mol)
$-PO_4$	-10.7 ± 1.1	2.37 ± 0.52	-11.1 ± 0.4	0	0
−Cit	-10.1 ± 0.4	2.89 ± 0.29	-9.65 ± 0.18	1.45 ± 0.44	1.98
$-AsO_4$	-10.5 ± 0.8	2.54 ± 0.46	-10.5 ± 0.20	0.58 ± 0.45	0.68
$-SO_4$	-9.63 ± 0.22	2.56 ± 0.15	-9.67 ± 0.09	1.43 ± 0.41	N/A

[a] Values obtained from the linear least-squares analysis of the data in Figure 4. Errors are the standard errors of fitting generated by Sigma-Plot. [b] Values are the average and standard deviation of at least 4 independent ΔG_f value determinations using eq 1 (see the text). [c] Values were obtained from the ΔG_{avg} values in column 4 and are relative to the PO_4 complex. [d] Values are taken from ref *14*.

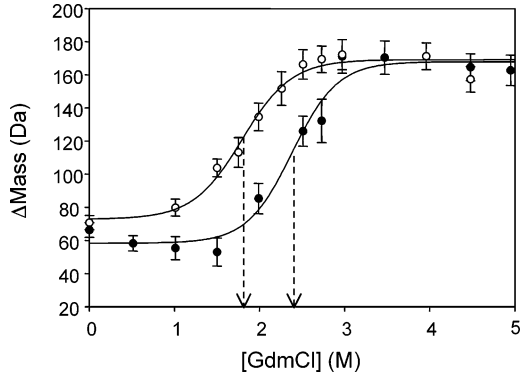

FIGURE 5: SUPREX curves recorded for Fe^{3+}FbpA$-PO_4$ (●) and Fe^{3+}FbpA−Cit (○) at pD 6.5 using an H/D exchange time of 1 h. The line represents the best fit of the data to a 4-parameter sigmoidal equation using Sigma-Plot. The error bars represent ±1 standard deviation. The $C_{SUPREX}^{1/2}$ value obtained for each curve, 2.38 ± 0.09 and 1.79 ± 0.06 M, respectively, is indicated with an arrow.

essentially the same. While the relative errors associated with the SUPREX-derived ΔG_f and m values in Table 2 are all reasonable, the relative errors associated with our m-value determinations (i.e., 6−22%) are generally larger than the relative errors associated with our ΔG_f values (i.e., ≤10%). The error associated with our m-value determinations appears to be random error; therefore, one way to reduce it would be to collect additional SUPREX curves at various times so that more than five points could be used in our linear least-squares analysis. Alternatively, because the m value is not expected to change for the different Fe^{3+}FbpA complexes in Table 2 (see above), the four data sets in Figure 4 could be used to generate an average m value for Fe^{3+}FbpA (i.e., the four m values reported in Table 2 could be averaged). Such a treatment of the data yields an average m value and standard deviation of 2.59 ± 0.22 kcal/(mol M).

With an established m value, it is possible to use eq 1 for the direct calculation of ΔG_f values from individual $C_{SUPREX}^{1/2}$ values. In this manner, five independent ΔG_f values can be determined from the $C_{SUPREX}^{1/2}$ values of the five different SUPREX curves that we recorded for each Fe^{3+}FbpA−X complex. Summarized in Table 2 are the average values (i.e., ΔG_{avg} value) and standard deviation of the ΔG_f values that were calculated in this manner for each Fe^{3+}FbpA−X complex in this study. We believe that these values better reflect the precision of our ΔG_f value measurements by SUPREX. It is also noteworthy that the $\Delta\Delta G_f$ values calculated using these ΔG_{avg} values are in good agreement with those previously reported in equilibrium exchange experiments (*14*). While a $\Delta\Delta G_f$ value for the Fe^{3+}-FbpA$-SO_4$ complex has not been reported previously, the binding affinity of SO_4 to iron-loaded FbpA has been qualitatively assessed to be less than that of PO_4 (*16*). The results reported here provide the first quantitative measurement of the binding affinity of this anion. Moreover, our results indicate that $\Delta\Delta G_f$ values greater than 1 kcal/mol can be readily determined by SUPREX on the FbpA system. This made it relatively straightforward to quantify the relative binding affinities of the synergistic anion in the Fe^{3+}FbpA−PO_4, Fe^{3+}FbpA−Cit, and Fe^{3+}FbpA$-SO_4$ complexes. But clearly, the anion-binding affinity in the Fe^{3+}FbpA$-AsO_4$ complex was too similar to that in the Fe^{3+}FbpA$-PO_4$ complex to be measured by SUPREX. A discussion of the structural and chemical basis for differential anion stabilization of the Fe^{3+}FbpA−X complexes studied here is found in ref *14*.

In conclusion, our results indicate that the SUPREX technique is amenable to the quantitative thermodynamic analysis of synergistic anion-binding interactions in the Fe^{3+}-FbpA−X system. This work represents the first example in which the SUPREX technique was used to evaluate $\Delta\Delta G_f$ values on a nontwo-state folding protein under EX1 exchange conditions. The general applicability of SUPREX for the quantitative thermodynamic analysis of protein−ligand-binding interactions in such "nonideal" protein systems in the SUPREX experiment remains to be determined. However, in the case of the Fe^{3+}FbpA−X system, the SUPREX-derived $\Delta\Delta G_f$ values reported here for Fe^{3+}FbpA$-PO_4$, Fe^{3+}FbpA$-AsO_4$, and Fe^{3+}FbpA−Cit were in good agreement with previously reported values (*14*). The SUPREX technique also enabled the first evaluation of a $\Delta\Delta G_f$ value for the synergistic anion, SO_4. Moreover, because the SUPREX method is applicable to impure samples containing mixtures of proteins, these studies represent important control experiments for future studies that will focus on the *ex vivo* analysis of the distribution of Fe^{3+}FbpA−X species in bacterial osmotic shock fluids enriched for Fe^{3+}FbpA. One hypothesis that has been set forth for periplasm−cytosol iron transport is that the anion bound by the Fe^{3+}FbpA−X complex will profoundly influence its lability for transport (*14*, *17*). Thus, our SUPREX approach shows promise for resolving this important biological question.

ACKNOWLEDGMENT

P. L. R. is grateful for financial support from a Duke Endowment Fellowship awarded to her by the Graduate School at Duke University, and K. D. W. is grateful for financial support from a NIH Biological Chemistry Training Grant (GM08558).

REFERENCES

1. Ghaemmaghami, S., Fitzgerald, M. C., and Oas, T. G. (2000) A quantitative, high-throughput screen for protein stability, *Proc. Natl. Acad. Sci. U.S.A. 97*, 8296−8301.

2. Ghaemmaghami, S., and Oas, T. G. (2001) Quantitative protein stability measurement *in vivo*, *Nat. Struct. Biol. 8*, 879−882.
3. Powell, K. D., Wales, T. E., and Fitzgerald, M. C. (2002) Thermodynamic stability measurements on multimeric proteins using a new H/D exchange- and matrix-assisted laser desorption/ionization (MALDI) mass spectrometry-based method, *Protein Sci. 11*, 841−851.
4. Powell, K. D., Wang, M. Z., Silinski, P., Ma, L., Wales, T. E., Dai, S. Y., Warner, A. H., Yang, X., and Fitzgerald, M. C. (2003) The accuracy and precision of a new H/D exchange- and mass spectrometry-based technique for measuring the thermodynamic stability of proteins, *Anal. Chim. Acta 496*, 225−232.
5. Powell, K. D., Ghaemmaghami, S., Wang, M. Z., Ma, L., Oas, T. G., and Fitzgerald, M. C. (2002) A general mass spectrometry-based assay for the quantitation of protein−ligand binding interactions in solution, *J. Am. Chem. Soc. 124*, 35, 10256−10257.
6. Powell, K. D., and Fitzgerald, M. C. (2003) Accuracy and precision of a new H/D exchange- and mass spectrometry-based technique for measuring the thermodynamic properties of protein−peptide complexes, *Biochemistry 42*, 4962−4970.
7. Powell, K. D., and Fitzgerald, M. C. (2001) Measurements of protein stability by H/D exchange and matrix-assisted laser desorption/ionization mass spectrometry using picomoles of material, *Anal. Chem. 73*, 3300−3304.
8. Ma, L., and Fitzgerald, M. C. (2003) A new H/D exchange- and mass spectrometry-based method for thermodynamic analysis of protein−DNA interactions, *Chem. Biol. 10*, 1205−1213.
9. Bai, Y., Milne, J. S., Mayne, L., and Englander, S. W.(1993) Primary structure effects on peptide group hydrogen exchange, *Proteins 17*, 75−86.
10. Mietzner, T. A., Tencza, S. B., Adhikari, P., Vaughan, K. G., and Nowalk, A. J. (1998) Periplasm-to-cytosol transporters of Gram-negative pathogens, *Curr. Top. Microbiol. Immunol. 225*, 114−135.
11. Bruns, C. M., Nowalk, A. J., Arvai, A. S., McTigue, M. A., Vaughan, K. C., Mietzner, T. A., and McRee, D. E. (1997) Structure of *Haemophilus influenzae* Fe^{3+}-binding protein reveals convergent evolution within a superfamily, *Nat. Struct. Biol. 4*, 919−924.
12. McRee, D. E., Bruns, C. M., Williams, P. A., Mietzner, T. A., and Nunn, R., to be published, PDB 1D9Y.
13. Taboy, C. H., Vaughan, K. G., Mietzner, T. A., Aisen, P., and Crumbliss, A. L. (2001) Fe^{3+} coordination and redox properties of a bacterial transferrin, *J. Biol. Chem. 276*, 2719−2724.
14. Dhungana, S., Taboy, C. H., Anderson, D. S., Vaughan, K. G, Aisen, P., Mietzner, T. A., and Crumbliss, A. L. (2003) The influence of the synergistic anion on iron chelation by ferric binding protein, a bacterial transferrin, *Proc. Nat. Acad. Sci. U.S.A. 100*, 3659−3664.
15. Guo, M., Harvey, I., Yang, W., Coghill, L., Campopiano, D. J., Parkinson, J. A., MacGillivray, R. T. A, Harris, W. R., and Sadler, P. J. (2003) Synergistic anion and metal binding to the ferric ion-binding protein from *Neisseria gonorrhoreae*, *J. Biol. Chem. 278*, 2490−2502.
16. Dhungana, S., Anderson, D. S., Mietzner, T. A., and Crumbliss, A. L. (2004) Phosphate ester hydrolysis is catalyzed by A bacterial transferrin: Potential implications for *in vivo* iron transport mechanisms, *J. Inorg. Biochem. 98*, 1975−1977.
17. Boukhalfa, H., Anderson, D. S., Mietzner, T. A., and Crumbliss, A. L. (2003) Kinetics and mechanism of iron release from the bacterial ferric binding protein nFbpA: Exogenous anion influence and comparison with mammalian transferrin, *J. Biol. Inorg. Chem. 8*, 881−892.
18. Gabričević, M., Anderson, D. S., Mietzner, T. A., and Crumbliss, A. L. (2004) Kinetics and mechanism of iron(III) complexation by ferric binding protein: The role of phosphate, *Biochemistry 43*, 5811−5819.
19. Ferguson, S. J. (1991) in *Prokaryotic Structure and Function: A New Perspecitve: 47th Symposium of the Society for General Microbiology* (Mohan, S., Dow, C., and Coles, J. A., Eds.) pp 311−339, Cambridge University Press, Edinburgh, U.K.
20. Nozaki, Y. (1972) The preparation of guanidine hydrochloride, *Methods Enzymol. 26*, 43−50.
21. Glasoe, P. K., and Long, F. A. (1960) Use of glass electrodes to measure acidities in deuterium oxide, *J. Phys. Chem. 64*, 188−190.
22. Mietzner, T. A., Bolan, G., Schoolnik, G. K., and Morse, S. A. (1987) Purification and characterization of the major iron-regulated protein expressed by pathogenic *Neisseriae*, *J. Exp. Med. 165*, 1041−1057.
23. Zhang, Y. Z. (1995) Protein and peptide structure and interactions studied by hydrogen exchange and NMR, Ph.D. Thesis, *Structural Biology and Molecular Biophysics*, University of Pennsylvania, PA.
24. Miranker, A., Robinson, C. V., Radford, C. E., Aplin, R. T. and Dobson, C. M. (1993) Detection of transient protein folding populations by mass spectrometry, *Science 262*, 896−900.
25. Smith, D. L., Deng, Y., and Zhang, Z. (1997) Probing the non-covalent structure of proteins by amide hydrogen exchange and mass spectrometry, *J. Mass Spectrom. 32*, 135−146.
26. Arrington, C. B., Teesch, L. M., and Robertson A. D. (1999) Defining protein ensembles with native-state NH exchange: Kinetics of interconversion and cooperative units from combined NMR and MS analysis, *J. Mol Biol. 285*, 1265−1275.
27. Myers, J. K., Pace, C. N., and Scholtz, J. M. (1995) Denaturant *m* values and heat capacity changes: Relation to changes in accessible surface area of protein unfolding, *Protein Sci.* 4, 2138−2148.

BI0481848